Journal Name

ARTICLE TYPE

Cite this: DOI: 10.1039/xxxxxxxxxx

How to quantify isotropic negative thermal expansion: magnitude, range, or both?†

Chloe S. Coates and Andrew L. Goodwin*

Negative thermal expansion (NTE) is the useful and counterintuitive material property of volume contraction on heating. Isotropic NTE is the rarest and most useful type, and is known to occur in a variety of different classes of materials. In this mini-review we ask the simple question of how best to compare NTE behaviour amongst these different systems? We summarise the two main mechanisms for isotropic NTE, and illustrate how these favour alternatively NTE magnitude and NTE range. We argue in favour of a combined metric of *NTE capacity*, which balances both effects and allows unbiased identification of the most remarkable NTE materials, irrespective of the underlying microscopic mechanism at play. By organising known NTE materials according to these various metrics, we find intuitive trends in behaviour that help identify key materials for specific NTE applications.

Introduction

Negative thermal expansion (NTE) is a counterintuitive phenomenon whereby a material shrinks, rather than expands, with increasing temperature.[1–5] It is allowed thermodynamically whenever a decrease in material volume couples to an increase in entropy.[5,6] The main applications of NTE—be they in dental fillings,[7,8] cooker hobs,[9] or high-precision optics[10]—rely on exploiting this thermal volume contraction to counteract the much more usual positive thermal expansion (PTE) of ordinary materials. Consequently there is a strong drive within the field to discover systems with increasingly extreme NTE characteristics—the argument being that the stronger the NTE, the easier it is to compensate PTE within these composite materials.[11–13]

What does it mean to say that NTE in one material is stronger than in another? Thermal expansion is usually quantified by the coefficient of thermal expansion

$$\alpha_V = \frac{1}{V}\frac{\partial V}{\partial T}, \qquad (1)$$

which reflects (obviously) the rate at which volume strain develops with temperature at constant pressure. Titanium, for example, has a coefficient of thermal expansion $\alpha_V \sim +27\,\mathrm{MK}^{-1}$.[14] This value is typical of many engineering materials and reflects a volume increase of about 0.3% for every 100 K. Zirconium tungstate, ZrW_2O_8, has always been a high-profile NTE material because $\alpha_V \sim -27\,\mathrm{MK}^{-1}$ over a large temperature range[3,15]—in other words, its NTE effect is about as large as the PTE effect in conventional materials.

But the notion of comparing thermal expansion characteristics in terms of a volume derivative (1) becomes meaningless wherever NTE occurs across a first-order phase transition. In such cases, there is a discontinuity in the $V(T)$ equation of state such that $\frac{\partial V}{\partial T}$—and hence α_V—diverges at some critical temperature T_c [Fig. 1]. By measuring molar volumes at sufficiently fine temperature intervals in the proximity of T_c it becomes possible to calculate values of α_V of arbitrarily large magnitude. So α_V alone cannot be a universal measure of the strength of NTE behaviour.

In practice, there are two key considerations when comparing the NTE performance of different materials. The first (and most frequently reported) is NTE magnitude as given by α_V and outlined above. But the second is the temperature range ΔT over which NTE is observed. This range is important because different applications will demand fundamentally different thermal operating windows for NTE. The high-precision optics on satellites, for example, experience repeated thermal cycling between −75 and +135 °C.[16,17] Whereas tooth enamel, by contrast, is exposed

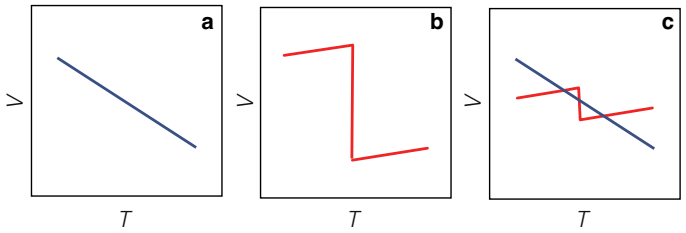

Fig. 1 Thermal contraction in NTE materials may occur (a) continuously, or (b) discontinuously. The coefficient of thermal expansion α_V depends on the slope of $V(T)$: infinite for (b) but finite for (a). How should we compare the degree of NTE represented by the two curves in (c)?

Department of Chemistry, University of Oxford, Inorganic Chemistry Laboratory, South Parks Road, Oxford OX1 3QR, U.K.; Tel: +44 1865 272137; E-mail: andrew.goodwin@chem.ox.ac.uk

† Electronic Supplementary Information (ESI) available: tabulated summary of known isotropic NTE materials and their NTE characteristics. See DOI: 10.1039/b000000x/

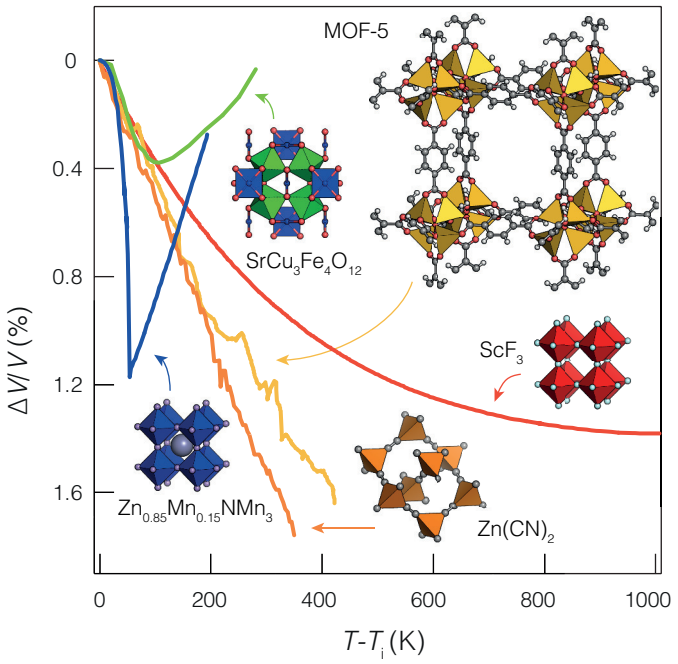

Fig. 2 Temperature-dependent volume strains in a variety of NTE materials: the magnetic antiperovskite $Zn_{0.85}Mn_{0.15}NMn_3$ (blue points);[18] the charge-transfer ceramic $SrCu_3Fe_4O_{12}$ (green points);[19] the metal–organic framework MOF-5 (yellow points);[20] anticuprite structured $Zn(CN)_2$ (orange points);[21] and the A-site-deficient perovskite ScF_3 (red points).[22] Data are given for temperatures relative to the onset temperature T_i of NTE.

only to a substantially narrower temperature range around 37 °C.

Fig. 2 shows some of the variety of thermal expansion behaviour observed experimentally for different types of NTE materials. Some systems, such as the antiperovskite $Zn_{0.85}Mn_{0.15}NMn_3$, show very abrupt NTE effects with a narrow ΔT. While others, such as ScF_3, show a much more gradual effect that nonetheless persists over a very broad temperature range. How should we understand such variety, and how should we best compare the NTE characteristics of these ostensibly very different systems?

There are, in practice, two fundamental mechanisms responsible for NTE that divide these various materials into two classes.[5,13,23,24] In the first class are materials for which NTE is driven by phonons; in the second are those for which NTE results from an electronic transition involving *e.g.* magnetic or charge order. In this mini-review we survey key materials in both groups, with the objective of comparing the magnitude and range of NTE in different systems. Our focus is entirely on crystalline materials with isotropic NTE—*i.e.* systems with cubic crystal symmetry. This choice facilitates comparison amongst different compounds, and also allows us to cast aside the role of elastic anisotropy that is crucial whenever NTE arises due from elastic coupling to PTE in other directions (*e.g.* in ferroelectrics and/or across ferroelastic phase transitions).[13,25,26] We will come to show that (i) phonon NTE mechanisms maximise ΔT, (ii) electronic-transition NTE mechanisms maximise the magnitude of α_V (albeit at the expense of ΔT), and (iii) an Ashby-style analysis[27,28] of various NTE materials partitions these systems naturally according to their underlying chemistry, with the most important NTE candidates emerging as those for which the product of $-\alpha_V$ and ΔT is largest.

Maximising range: phonon-mediated NTE

Phonon-mediated NTE is the dominant mechanism amongst network materials; *i.e.* open structures with directional covalent bonding.[5,23] The canonical system of this type is ZrW_2O_8.[3,29] On the very simplest level, its NTE is driven by transverse vibrations of Zr–O–W linkages: displacement of the O atom away from the Zr…W axis reduces the distance between Zr and W atoms, and hence the overall volume. This local mechanism is sometimes called the 'tension effect',[30] and is implicated in one form or another in nearly all phonon-mediated NTE materials. In the case of ZrW_2O_8, local transverse displacements couple together to give a particularly complex set of NTE phonons,[31–33] such that the collective mechanism for NTE involves a combination of translations, rotations, and deformations of ZrO_6 and WO_4 polyhedra towards a denser state.[34,35] A simpler but conceptually-related mechanism operates in ScF_3, where the key NTE phonons involve correlated rotations of connected ScF_6 octahedra [Fig. 3].

Whatever their particular form, NTE phonons have a clear thermodynamic signature in that their associated Grüneisen parameter[36]

$$\gamma = -\frac{\partial \ln \omega}{\partial \ln V} \tag{2}$$

is negative; here ω is the (angular) mode frequency. If $\gamma < 0$ then vibrational energies decrease with decreasing volume: this is what links volume contraction to an increase in vibrational mode population, and hence vibrational entropy.[5] The formal relation to thermal expansion comes *via*

$$\alpha_V(T) = \frac{1}{BV}\sum_i \gamma_i C_{V,i}(T), \tag{3}$$

where B is the bulk modulus, and the mode Grüneisen parameters γ_i are weighted by their contributions $C_{V,i}(T)$ to the constant-volume heat capacity.[5,37,38] So already we can expect that NTE should be strongest for soft materials (low B), and where there are many low-energy (high C_V) NTE phonon modes with large and negative γ. Moreover, we can identify the temperature range over which one expects to observe NTE as that for which NTE modes dominate the $\gamma_i C_{V,i}(T)$ sum in Eq. (3). In systems for which the low-energy phonon spectrum is almost exclusively charac-

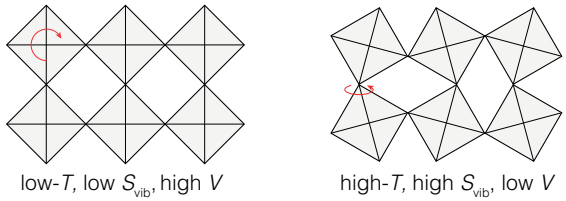

Fig. 3 A simplified representation of phonon-mediated NTE in open-framework materials such as ScF_3. NTE phonon modes often involve correlated rotations of connected polyhedral units that act to reduce the material volume.

terised by NTE modes, this temperature range may be expected to span many hundreds—or even thousands—of degrees Kelvin.

Some of the earliest examples of phonon-mediated NTE materials include families of transition-metal oxides, which display moderate NTE of a similar magnitude to conventional positive thermal expansion materials. The structures of these various systems tend to consist of corner-sharing polyhedra: for example, corner-sharing tetrahedra in the β-cristobalite polymorph of SiO_2 ($\alpha_V = -6.9(6)\,MK^{-1}$),[39] octahedra in ReO_3 ($\alpha_V = -3(3)\,MK^{-1}$),[40,41] and a combination of the two in ZrW_2O_8 ($\alpha_V = -26.1\,MK^{-1}$).[34,42] As we have already seen, the fluoride perovskite ScF_3 is structurally similar, and its NTE ($\alpha_V = -12.3\,MK^{-1}$) persists from 10 to 1000 K.[22] Zeolites—with their open network structures assembled from corner-linked AlO_4 and SiO_4 tetrahedra—are another relevant family of this type, and many of these technologically important materials do indeed show NTE.[43,44] The key point here is that many open-framework oxide/fluoride frameworks tend to show moderate NTE ($\alpha_V \simeq -10\,MK^{-1}$; the moderacy itself reflecting the stiffness of metal–O/F interactions and thus a larger B), but this NTE can be sustained over a large temperature range, with $\langle \Delta T \rangle = 375$ K.

There are two important ramifications of replacing the monatomic M–O/F–M linkages of these ceramic NTE materials with molecular anionic linkers, such as in $Zn(CN)_2$ or the broad family of metal–organic frameworks (MOFs). The first is that the number of phonon modes with NTE characteristics increases; this has the effect of amplifying the sum in Eq. (3). The second is that molecular frameworks tend to contain more open space, and as such are more flexible; this has the effect of reducing the elastic stiffness as measured by B. Both effects make α_V increasingly negative, and so one anticipates increasingly strong NTE behaviour in molecular framework materials with open structures.

This expectation is indeed borne out in practice. A good example is that of $Zn(CN)_2$, the diamondoid structure of which is closely related to that of β-cristobalite.[21,45–47] Whereas NTE modes in the latter involve only counter-rotation of neighbouring tetrahedra,[48,49] the former has access to a broad spectrum of NTE modes extending well beyond the cristobalite modes to include same-sense-rotations and rigid-unit translations.[21,50–52] This difference in density of NTE modes translates to an order-of-magnitude increase in α_V.[53] Further enhancement occurs in the series of solid solutions of $Zn_xCd_{1-x}(CN)_2$. Here, the larger mass of Cd serves lowers the NTE phonon energies, which in turn increases the $C_{V,i}$, and hence the magnitude of α_V.[54–56] The related family of Prussian Blue analogues (PBAs) represents the molecular framework analogue of A-site-deficient perovskites such as ScF_3.[57,58] Again, NTE in PBAs is well documented;[59–64] by varying composition it is possible to obtain coefficients of thermal expansion that vary between $-4.41\,MK^{-1}$ for $FeCo(CN)_6$ and as much as $-120(18)\,MK^{-1}$ in $Zn_3[Fe(CN)_6]_2$.[59,64] Such extreme values are accessed by including a substantial fraction of site vacancies, a strategy that is known to enhance further the density of NTE modes.[41,53]

MOFs are an excellent example of open-framework materials with large void fractions and low bulk moduli;[65] indeed systems with fractional pore volumes as large as $\sim 90\%$ are not unknown.[66,67] So it is perhaps unsurprising that the canonical MOF-5 shows pronounced NTE ($\alpha_V = -39.3(3)\,MK^{-1}$) which persists over its entire stability window $80 \leq T \leq 500$ K [Fig. 2].[20] Or that a number of other high-symmetry MOFs (*e.g.* MOF-14,[68] HKUST-1,[69] and UiO-66[70,71]) also show the effect—either experimentally[20,68,69,71] or as determined computationally using *e.g. ab initio* calculations.[72–74] Again the concept of tuning NTE *via* defect engineering has been demonstrated for MOFs, except that in the case of UiO-66 it appears (bizarrely) that increasing vacancy contributions lead to a reduction in magnitude of NTE. Whatever the mechanism for this may be, an important general corollary of the weaker bonding in MOFs that can limit their usefulness as NTE materials is their inherent instability with respect to phase transitions (*e.g.* low shear moduli) and/or their tendency to decompose thermally.[75–77] So, although the magnitude of α_V is usually enhanced in these systems relative to the ceramics discussed above, the temperature window for NTE is often reduced.

Maximising magnitude: NTE from electronic transitions

The limiting case of increasing the magnitude of α_V at the expense of the NTE temperature window ΔT is one where volume contraction occurs on heating through a phase transition [Fig. 1(b)]. As we (and others[12,13,78]) have already flagged, the value of α_V necessarily diverges—irrespective of whether the transition is first- or second-order—and at the same time ΔT becomes infinitesimally small. A key requirement for such a transition is the stabilisation of a distinct high-entropy low-volume phase [Fig. 4]. Here we consider briefly the two primary examples of such a transition in the NTE literature: magnetic-order-driven volume expansion on cooling, on the one hand, and charge-transfer transitions, on the other hand.[13,79]

Magnetostriction

In certain magnetic materials, there is a volume expansion associated with the onset of magnetic ordering on cooling.[80,81] Known as the magnetovolume effect (MVE),[81–83] this coupling between magnetic and lattice degrees of freedom may even be exploitable in magnetic refrigeration technologies.[84] Perhaps the most widely studied family of MVE/NTE materials is that based on the antiperovskite manganese nitrides, $ANMn_3$; here A is usually a transition metal, metalloid or rare earth metal.[85,86] The

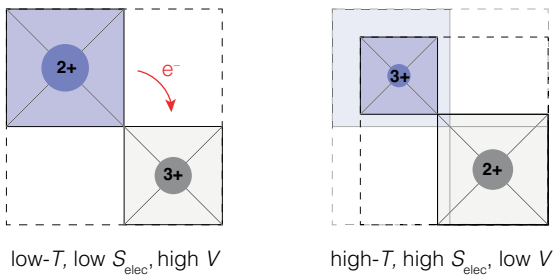

Fig. 4 A simplified representation of charge-transfer-mediated NTE in systems such as $LaCu_3Fe_4O_{12}$. The high-temperature low-volume state is stabilised by an increased electronic entropy.

structure consists of corner-sharing NMn_6 octahedra with the A metal occupying the A-site of conventional perovskites [Fig. 2]. In many of these systems—including *e.g.* $AgNMn_3$—the first-order magnetic transition that occurs on cooling (possibly ferro- or antiferromagnetic depending on the nature of A) is accompanied by a marked isotropic volume expansion. Such behaviour is understood in terms of the competition between itineracy at high temperatures (large electronic entropy, increased orbital overlap from smaller Mn…Mn distances) and magnetism at low temperatures (low entropy, stronger electron localisation from larger Mn…Mn distances).[87–92]

These magnetostriction-driven NTE systems are typified by extremely large, and even 'colossal' values of α_V over fairly narrow temperature ranges. For example, thermal expansion data for $Zn_{0.85}Mn_{0.15}NMn_3$ are shown in blue in Fig. 2; for this system $\alpha_V = -174.6\,MK^{-1}$ between 94 and 155 K.[18] The phase transition window associated with NTE can be extended at the expense of α_V by diluting the magnetic ions with a non-magnetic species (or, alternatively, by introducing competing ferromagnetic interactions as in Ref. 93).[92,94] In the specific case of $Zn_{1-x}Mn_xNMn_3$, increasing x to 0.3 allows ΔT to be broadened to 98 K, with a threefold reduction in the coefficient of thermal expansion for ($\alpha_V = -49.5\,MK^{-1}$). A similar strategy employed in related systems is to substitute N for either C or B.[85,95] Chemical doping can even change the nature of the phase transition itself. For example, in the $La(Fe/Co,Si/Al)_{13}$ family, exchange of Fe for Co or of Si for Al gradually shifts the phase transition type from second-order antiferromagnetic to first-order ferromagnetic.[96,97] This has the effect in $La(Fe_{1-x}Co_x)_{11.4}Al_{1.6}$ of extending ΔT from 152 to 190 K while α_V is reduced in magnitude from -50 to $-39\,MK^{-1}$.[97]

Charge-transfer materials

Phase transitions involving the redistribution of valence electrons can also give rise to conceptually similar NTE effect. Such transitions might include localised charge transfer between metal centres[19,98–100] or valence transitions in rare-earth compounds.[101–103] In both cases, volume contraction on heating is caused by changes in equilibrium bond lengths of the different valence states. For example, $LaCu_3Fe_4O_{12}$ exhibits a first-order charge-transfer transition on cooling:[104,105]

$$3Cu^{2+} + 4Fe^{3.75+} \rightarrow 3Cu^{3+} + 4Fe^{3+}.$$

The change in Fe–O bond lengths associated with transition are larger than those of the Cu–O bonds, and so the high-temperature $Cu^{2+}/Fe^{3.75+}$ configuration has a reduced molar volume.[104] Gradual chemical substitution of Fe for Mn effectively relaxes the first-order transition such that the NTE becomes more moderate ($\alpha_V = -66\,MK^{-1}$) and spans the wider T-range $300 \leq T \leq 340$ K in $LaCu_3Fe_{3.25}Mn_{0.75}O_{12}$.[98] On exchanging La completely for Sr, the transition becomes intrinsically second-order giving $\alpha_V = -40.23\,MK^{-1}$ across the range $170 \leq T \leq 270$ K.[19] Thermal expansion data for $SrCu_3Fe_4O_{12}$ are shown in green in Fig. 2, with pronounced contraction occurring over a more limited range than the phonon NTE materials.

Valence-state charge transfer transitions can also drive NTE in a conceptually similar manner. For example, in $YbInCu_4$ the variation in formal f-electron count at 66.9 K gives rise to a large molar volume at low temperatures (localised electrons, formal Yb charge 2.9+, longer bonds) than at temperatures above 67 K (delocalised electrons, formal Yb charge 3.0+, shorter bonds). Experimental lattice-parameter measurements across the transition give $\alpha_V = -57.9\,MK^{-1}$ across the temperature range $8 \leq T \leq 90$ K).[101] In the related material $Sm_{1-x}Y_xS$—a 'heavy fermion' Kondo insulator—α_V reaches $-96.9\,MK^{-1}$ between $9 \leq T \leq 250$ K for $x = 0.33$. The Sm electrons gradually localise from the conduction band on cooling as $Sm^{3+} \rightarrow Sm^{2+}$, leading to expansion of the unit cell.[102]

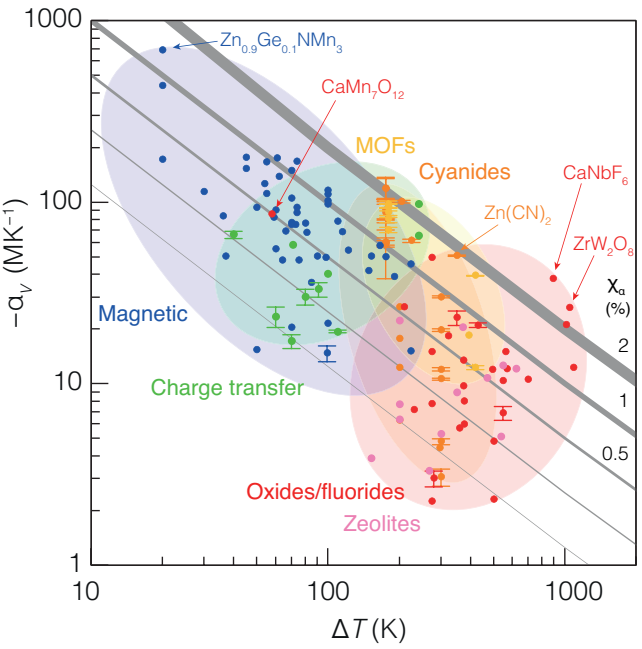

Fig. 5 Ashby-type plot of NTE characteristics for experimentally-studied isotropic NTE materials. Diagonal lines link points of constant NTE capacity $\chi_\alpha = \Delta V/V = -\alpha_V \Delta T$. Individual data points are coloured according to the corresponding chemical family and NTE mechanism.

Magnitude *and* range: NTE capacity

So we have seen that electonic-transition-mediated NTE materials tend to have larger values of $|\alpha_V|$ but smaller ΔT than phonon-mediated systems. But is either mechanism intrinsically *better*? Hence we return to the initial question we had hoped to address: how might we hope to meaningfully compare these different behaviours?

In Fig. 5 we present an 'Ashby plot' of the relationship between experimental values of $-\alpha_V$ and ΔT for the large number of isotropic NTE materials studied to date.[27] These data fall naturally along a diagonal, reflecting the observation that the product of the two parameters $-\alpha_V \Delta T$ is mostly preserved even amongst this large collection of very different systems. This product has a clear physical meaning: it is a dimensionless quantity that corresponds to the relative volume contraction $\Delta V/V$ exhibited by a material over the temperature range for which it exhibits NTE. By analogy to the 'compressibility capacity' metric χ_K introduced in

the context of negative linear compressibility (NLC) materials,[28] we suggest the term 'NTE capacity' and the symbol χ_α to denote this value. Evidently, for the vast majority of NTE materials—irrespective of underlying mechanism or system chemistry—the value of α_V falls between 0.1 and 1.0%. At the extreme of large $-\alpha_V$ lie the dense phase-transition-type NTE materials; at the other extreme, with large values of ΔT, lie the phonon-driven NTE materials with their open framework structures. Even amongst these framework systems, one observes a sensible trend in terms of pore fraction and bonding strength, reflecting the various differences in α_V and ΔT rationalised above for MOFs *vs* cyanides *vs* oxides.

A particular success of this representation is its ability to help distinguish the truly remarkable NTE compounds within ostensibly different families: they are the materials for which the value of χ_α is maximised—*i.e.* they tend toward the top-right corner of the plot in Fig. 5. So, for instance, amongst the MVE antinitrides, $Zn_{0.9}Ge_{0.1}NMn_3$ is clearly exceptional, not just because its measured coefficient of thermal expansion is so large and negative, but because it exhibits a total volume contraction of 1.4%, which is larger than that of the vast majority of other NTE materials.[106] Likewise, canonical NTE systems long known to be important in the field—such as ZrW_2O_8 and $Zn(CN)_2$—are easily identifiable in terms of their large NTE capacities.[3,21,46]

We make three further observations regarding the data in Fig. 5. First, the value of ΔT for a given system is often limited by the variable-temperature capabilities of experimental tools at hand. This is a particularly relevant point for phonon-mediated NTE in MOFs and cyanides, which is historically studied over the temperature range 100–295 K: these are the temperatures most readily accessed by in-house single-crystal X-ray diffraction measurements. Note the large number of MOF and cyanide data points with the same $\Delta T \simeq 195$ K. In nearly all cases, these systems would be expected to show NTE both to lower and to higher temperatures than probed experimentally so far, and so more extensive measurements would likely translate these data points further to the right of the plot; *i.e.* their NTE capacities are likely underestimated in our analysis. The second point concerns the effect of substitutional 'broadening' of NTE behaviour in magnetic and electronic-transition-driven systems.[95] Here one finds that a substitutional family lies along a single diagonal, with the parent compound at the top-left, and its substituted derivatives progressively arranged towards the bottom-right direction. In other words, substitution has very little effect on χ_α, but allows the chemist to navigate the constant-capacity diagonals in Fig. 5. And, finally, we argue it is possible to identify anomalous assignments of NTE mechanisms in existing studies. Take, for instance, the compound $CaMn_7O_{12}$, which is thought to exhibit NTE *via* a phonon-mediated mechanism;[107] its location within the Ashby plot suggests that a magnetic or electronic instability is the more likely mechanism. Perhaps this system deserves revisiting?

Concluding remarks

While the phenomenology and underlying mechanisms of NTE have been reviewed excellently many times previously[4,5,11,13,23,24,78,108–110]—and certainly in much greater depth than we achieve here—we feel our key contribution in this minireview to be the compilation of data in Fig. 5; the numerical values used to generate this plot are provided as supporting information. Our hope, of course, is that this representation will help the community identify a number of key compounds or classes of materials for future investigations. Ashby plots, such as ours, are especially useful in selecting materials optimised for a particular application. For example, if ΔT is required for some specific exploitation of NTE, then clearly phonon-mediated systems are the systems of choice. By contrast, MVE materials are the best candidates for extreme NTE localised within a narrow temperature window. We suggest that the most exciting area for future research is the region of the Ashby plot for which χ_α is maximised: those systems for which both $-\alpha_V$ and ΔT are maximal. Our data suggest that MOFs and cyanide frameworks are the currently-known systems most likely to occupy this space, especially if experimental measurements are extended to wider temperature ranges.

Years ago, we suggested (somewhat tongue-in-cheek, and in the context of anisotropic NTE materials) that systems with $\alpha < -100\,\mathrm{MK}^{-1}$ might be termed 'colossal' NTE materials.[61] The arguments we develop here—as others have elsewhere[13,78]—expose the inevitable futility of such a definition. What is obviously more meaningful is to highlight systems with particularly large NTE capacities, say $\chi_\alpha \geq 2\%$. Certainly, extremely few such systems are known to date, and those that are known are excellent representatives of the extreme physics accessible to a particular NTE mechanism or material chemistry. But the NTE community should presumably also set its sights high for the future: can we ever make a (gargantuan?) NTE material with $\chi_\alpha > 10\%$? Such a material would clearly have to be fundamentally different to those NTE systems identified so far, driven by an entirely new type of NTE physics. Whatever this physics may be, what seems likely is that any such material is most likely to be discovered by seeking to optimise at once *both* NTE magnitude *and* NTE range.

Conflicts of interest

There are no conflicts to declare.

Acknowledgements

The authors gratefully acknowledge financial support from the Leverhulme Trust (Grant No. RPG-2015-292), and thank A. B. Cairns (Imperial College London) and H. H. M. Yeung (Oxford) for useful discussions.

References

1 M. Blackman, *Phil. Mag.*, 1958, **3**, 831–838.
2 C. N. Chu, N. Saka and N. P. Suh, *Mater. Sci. Eng.*, 1987, **95**, 303–308.
3 T. A. Mary, J. S. O. Evans, T. Vogt and A. W. Sleight, *Science*, 1996, **272**, 90–92.
4 J. S. O. Evans, *J. Chem. Soc., Dalton Trans.*, 1999, **19**, 3317–3326.
5 M. T. Dove and H. Fang, *Rep. Prog. Phys.*, 2016, **79**, 066503.

6 M. J. Klein and R. D. Mountain, *J. Phys. Chem. Solids*, 1962, **23**, 425–427.

7 A. Versluis, W. H. Douglas and R. L. Sakaguchi, *Dent. Mater.*, 1996, **12**, 290–294.

8 M. B. Jakubinek, C. O'Neill, C. Felix, R. B. Price and M. A. White, *Dent. Mater.*, 2008, **24**, 1468–1476.

9 W. Pannhorst, *J. Non-Cryst. Solids*, 1997, **219**, 198–204.

10 D. A. Fleming, D. W. Johnson and P. J. Lemaire, *Article Comprising a Temperature Compensated Optical Fiber Refractive Index Grating*, U.S. Patent 5,694,503, 1997.

11 C. P. Romao, K. J. Miller, C. A. Whiteman and M. A. White, *Negative thermal expansion (thermomiotic) materials*, Amsterdam: Elsevier, 2013.

12 K. Takenaka, *Sci. Technol. Adv. Mater.*, 2012, **13**, 013001.

13 J. Chen, L. Hu, J. Deng and X. Xing, *Chem. Soc. Rev.*, 2015, **44**, 3522–3567.

14 P. Hidnert, *J. Res. Natl. Bur. Std.*, 1943, **30**, 101–105.

15 G. Ernst, C. Broholm, G. R. Kowach and A. P. Ramirez, *Nature*, 1998, **396**, 147–149.

16 D. Zhengchun, Z. Mengrui, W. Zhiguo and Y. Jianguo, *Compos. Struct.*, 2016, **152**, 693–703.

17 R. Jassemi-Zargani and J. F. Simard, 2nd CanSmart Workshop, 1999.

18 J. Lin, P. Tong, W. Tong, Y. Zou, C. Yang, F. Zhu, X. Zhang, L. Li, M. Wang, Y. Wu, S. Lin, W. Song, X. Zhu and Y. Sun, *Scripta Mater.*, 2018, **152**, 6–10.

19 Y. Ikuya, T. Kazuki, O. Kenya, H. Naoaki, K. Jungeun, T. Naruki, T. Ryoji, M. Masafumi, N. Norimasa, I. Toru, I. Tetsuo, K. Kenichi, T. Masaki and T. Mikio, *Angew. Chem. Int. Ed.*, 2011, **50**, 6579–6582.

20 N. Lock, Y. Wu, M. Christensen, L. J. Cameron, V. K. Peterson, A. J. Bridgeman, C. J. Kepert and B. B. Iversen, *J. Phys. Chem. C*, 2010, **114**, 16181–16186.

21 A. L. Goodwin and C. J. Kepert, *Phys. Rev. B*, 2005, **71**, 140301.

22 B. K. Greve, K. L. Martin, P. L. Lee, P. J. Chupas, K. W. Chapman and A. P. Wilkinson, *J. Am. Chem. Soc.*, 2010, **132**, 15496–15498.

23 R. Mittal, M. Gupta and S. Chaplot, *Prog. Mater. Sci.*, 2018, **92**, 360 – 445.

24 W. Miller, C. W. Smith, D. S. Mackenzie and K. E. Evans, *J. Mater. Sci.*, 2009, **44**, 5441–5451.

25 I. M. Shmyt'ko, N. S. Afonikova and V. I. Torgashev, *Phys. Solid State*, 2002, **44**, 2309–2317.

26 J. Chen, X. Xing, R. Yu and G. Liu, *J. Am. Ceram. Soc.*, 2005, **88**, 1356–1358.

27 M. F. Ashby, *Materials selection in mechanical design*, Butterworth-Heinemann, Cambridge, 5th edn, 2016.

28 A. B. Cairns and A. L. Goodwin, *Phys. Chem. Chem. Phys.*, 2015, **17**, 20449–20465.

29 J. S. O. Evans, T. A. Mary, T. Vogt, M. A. Subramanian and A. W. Sleight, *Chem. Mater.*, 1996, **8**, 2809–2823.

30 T. H. K. Barron and K. J. Rogers, *Mol. Simul.*, 1989, **4**, 27–35.

31 J. N. Hancock, C. Turpen, Z. Schlesinger, G. R. Kowach and A. P. Ramirez, *Phys. Rev. Lett.*, 2004, **93**, 225501.

32 V. Gava, A. L. Martinotto and C. A. Perottoni, *Phys. Rev. Lett.*, 2012, **109**, 195503.

33 A. Sanson, *Chem. Mater.*, 2014, **26**, 3716–3720.

34 A. K. A. Pryde, K. D. Hammonds, M. T. Dove, V. Heine, J. D. Gale and M. C. Warren, *J. Phys.: Condens. Matter*, 1996, **8**, 10973.

35 M. Baise, P. M. Maffettone, F. Trousselet, N. P. Funnell, F.-X. Coudert and A. L. Goodwin, *Phys. Rev. Lett.*, 2018, **120**, 265501.

36 E. Grüneisen, *Ann. Phys.*, 1912, **344**, 257–306.

37 R. H. Baughman, *J. Chem. Phys.*, 1973, **58**, 2976–2983.

38 T. Barron, J. Collins and G. White, *Adv. Phys.*, 1980, **29**, 609–730.

39 E. Bourova and P. Richet, *Geophys. Res. Lett.*, 1998, **25**, 2333–2336.

40 T. Chatterji, P. F. Henry, R. Mittal and S. L. Chaplot, *Phys. Rev. B*, 2008, **78**, 134105.

41 E. E. Rodriguez, A. Llobet, T. Proffen, B. C. Melot, R. Seshadri and P. B. Littlewood, *J. Appl. Phys.*, 2009, **105**, 114901.

42 M. G. Tucker, A. L. Goodwin, M. T. Dove, D. A. Keen, S. A. Wells and J. S. O. Evans, *Phys. Rev. Lett.*, 2005, **95**, 255501.

43 P. Lightfoot, D. A. Woodcock, M. J. Maple, L. A. Villaescusa and P. A. Wright, *J. Mater. Chem.*, 2001, **11**, 212–216.

44 K. D. Hammonds, V. Heine and M. T. Dove, *J. Phys. Chem. B*, 1998, **102**, 1759–1767.

45 B. F. Hoskins and R. Robson, *J. Am. Chem. Soc.*, 1990, **112**, 1546–1554.

46 D. J. Williams, D. E. Partin, F. J. Lincoln, J. Kouvetakis and M. O'Keeffe, *J. Solid State Chem.*, 1997, **134**, 164–169.

47 I. P. Swainson and M. T. Dove, *Phys. Chem. Minerals*, 1995, **22**, 61–65.

48 I. P. Swainson and M. T. Dove, *Phys. Rev. Lett.*, 1993, **71**, 193–196.

49 S. A. Wells, M. T. Dove, M. G. Tucker and K. Trachenko, *J. Phys.: Condens. Matter*, 2002, **14**, 4645.

50 K. W. Chapman, P. J. Chupas, and C. J. Kepert, *J. Am. Chem. Soc.*, 2005, **127**, 15630–15636.

51 S. J. Hibble, A. M. Chippindale, E. Marelli, S. Kroeker, V. K. Michaelis, B. J. Greer, P. M. Aguiar, E. J. Bilbé, E. R. Barney and A. C. Hannon, *J. Am. Chem. Soc.*, 2013, **135**, 16478–16489.

52 H. Fang, M. T. Dove, L. H. N. Rimmer and A. J. Misquitta, *Phys. Rev. B*, 2013, **88**, 104306.

53 A. L. Goodwin, *Phys. Rev. B*, 2006, **74**, 134302.

54 V. E. Fairbank, A. L. Thompson, R. I. Cooper and A. L. Goodwin, *Phys. Rev. B*, 2012, **86**, 104113.

55 P. Ding, E. J. Liang, Y. Jia and Z. Y. Du, *J. Phys.: Condens. Matter*, 2008, **20**, 275224.

56 J. W. Zwanziger, *Phys. Rev. B*, 2007, **76**, 052102.

57 J. Brown, *Philosoph. Trans.*, 1724, **33**, 17–24.

58 M. B. Zakaria and T. Chikyow, *Coord. Chem. Rev.*, 2017, **352**,

328–345.
59 S. Margadonna, K. Prassides and A. N. Fitch, *J. Am. Chem. Soc.*, 2004, **126**, 15390–15391.
60 A. L. Goodwin, K. W. Chapman and C. J. Kepert, *J. Am. Chem. Soc.*, 2005, **127**, 17980–17981.
61 A. L. Goodwin, D. A. Keen, M. G. Tucker, M. T. Dove, L. Peters and J. S. O. Evans, *J. Am. Chem. Soc.*, 2008, **130**, 9660–9661.
62 K. W. Chapman, P. J. Chupas and C. J. Kepert, *J. Am. Chem. Soc.*, 2006, **128**, 7009–7014.
63 T. Matsuda, J. E. Kim, K. Ohoyama and Y. Moritomo, *Phys. Rev. B*, 2009, **79**, 172302.
64 S. Adak, L. L. Daemen, M. Hartl, D. Williams, J. Summerhill and H. Nakotte, *J. Solid State Chem.*, 2011, **184**, 2854–2861.
65 J. C. Tan and A. K. Cheetham, *Chem. Soc. Rev.*, 2011, **40**, 1059–1080.
66 H. Furukawa, N. Ko, Y. B. Go, N. Aratani, S. B. Choi, E. Choi, A. Ö. Yazaydin, R. Q. Snurr, M. O'Keeffe, J. Kim and O. M. Yaghi, *Science*, 2010, **329**, 424–428.
67 J. K. Schnobrich, K. Koh, K. N. Sura and A. J. Matzger, *Langmuir*, 2010, **26**, 5808–5814.
68 Y. Wu, V. K. Peterson, E. Luks, T. A. Darwish and C. J. Kepert, *Angew. Chem. Int. Ed.*, 2014, **53**, 5175–5178.
69 Y. Wu, A. Kobayashi, G. Halder, V. Peterson, K. Chapman, N. Lock, P. Southon and C. Kepert, *Angew. Chem. Int. Ed.*, 2008, **47**, 8929–8932.
70 M. J. Cliffe, W. Wan, X. Zou, P. A. Chater, A. K. Kleppe, M. G. Tucker, H. Wilhelm, N. P. Funnell, F.-X. Coudert and A. L. Goodwin, *Nat. Commun.*, 2014, **5**, 4176.
71 M. J. Cliffe, J. A. Hill, C. A. Murray, F.-X. Coudert and A. L. Goodwin, *Phys. Chem. Chem. Phys.*, 2015, **17**, 11586–11592.
72 D. Dubbeldam, K. Walton, D. Ellis and R. Snurr, *Angew. Chem. Int. Ed.*, 2007, **46**, 4496–4499.
73 F.-X. Coudert, *Chem. Mater.*, 2015, **27**, 1905–1916.
74 S. R. G. Balestra, R. Bueno-Perez, S. Hamad, D. Dubbeldam, A. R. Ruiz-Salvador and S. Calero, *Chem. Mater.*, 2016, **28**, 8296–8304.
75 J. C. Tan, B. Civalleri, C.-C. Lin, L. Valenzano, R. Galvelis, P.-F. Chen, T. D. Bennett, C. Mellot-Draznieks, C. M. Zicovich-Wilson and A. K. Cheetham, *Phys. Rev. Lett.*, 2012, **108**, 095502.
76 A. U. Ortiz, A. Boutin, A. H. Fuchs and F.-X. Coudert, *Phys. Rev. Lett.*, 2012, **109**, 195502.
77 P. Küsgens, M. Rose, I. Senkovska, H. Fröde, A. Henschel, S. Siegle and S. Kaskel, *Micro. Meso. Mater.*, 2009, **120**, 325–330.
78 K. Takenaka, *Front. Chem.*, 2018, **6**, 267.
79 M. Azuma, K. Oka and K. Nabetani, *Sci. Technol. Adv. Mater.*, 2015, **16**, 034904.
80 C. E. Guillaume, *C. R. Acad. Sci.*, 1897, **125**, 235–238.
81 G. Hausch, *Phys. Stat. Sol. A*, 1973, **18**, 735–740.
82 R. J. Weiss, *Proc. Phys. Soc.*, 1963, **82**, 281.
83 A. Katsuki and K. Terao, *J. Phys. Soc. Jap.*, 1969, **26**, 1109–1114.
84 S. Fähler and V. K. Pecharsky, *MRS Bull.*, 2018, **43**, 264–268.
85 T. Hamada and K. Takenaka, *J. Appl. Phys.*, 2011, **109**, 07E309.
86 T. Peng, W. Bo-Sen and S. Yu-Ping, *Chin. Phys. B*, 2013, **22**, 067501.
87 P. L'Heritier, D. Boursier and R. Fruchart, *Mater. Res. Bull.*, 1981, **16**, 1511–1519.
88 B. Y. Qu and B. C. Pan, *J. Appl. Phys.*, 2010, **108**, 113920.
89 K. Kodama, S. Iikubo, K. Takenaka, M. Takigawa, H. Takagi and S. Shamoto, *Phys. Rev. B*, 2010, **81**, 224419.
90 D. Tahara, Y. Motome and M. Imada, *J. Phys. Soc. Jap.*, 2007, **76**, 013708.
91 S. Iikubo, K. Kodama, K. Takenaka, H. Takagi and S. Shamoto, *Phys. Rev. B*, 2008, **77**, 020409.
92 K. Takenaka, M. Ichigo, T. Hamada, A. Ozawa, T. Shibayama, T. Inagaki and K. Asano, *Sci. Technol. Adv. Mater.*, 2014, **15**, 015009.
93 X. Guo, P. Tong, J. Lin, C. Yang, K. Zhang, S. Lin, W. Song and Y. Sun, *Front. Chem.*, 2018, **6**, 75.
94 J. C. Lin, P. Tong, W. Tong, S. Lin, B. S. Wang, W. H. Song, Y. M. Zou and Y. P. Sun, *Appl. Phys. Lett.*, 2015, **106**, 082405.
95 K. Takenaka and H. Takagi, *Appl. Phys. Lett.*, 2005, **87**, 261902.
96 R. Huang, Y. Liu, W. Fan, J. Tan, F. Xiao, L. Qian and L. Li, *J. Am. Chem. Soc.*, 2013, **135**, 11469–11472.
97 Y. Zhao, R. Huang, S. Li, W. Wang, X. Jiang, Z. Lin, J. Li and L. Li, *Phys. Chem. Chem. Phys.*, 2016, **18**, 20276–20280.
98 I. Yamada, S. Marukawa, M. Murakami and S. Mori, *Appl. Phys. Lett.*, 2014, **105**, 231906.
99 I. Yamada, S. Marukawa, N. Hayashi, M. Matsushita and T. Irifune, *Appl. Phys. Lett.*, 2015, **106**, 151901.
100 I. Yamada, K. Shiro, N. Hayashi, S. Kawaguchi, T. Kawakami, R. Takahashi and T. Irifune, *J. Asian Ceram. Soc.*, 2017, **5**, 169–175.
101 B. Kindler, D. Finsterbusch, R. Graf, F. Ritter, W. Assmus and B. Lüthi, *Phys. Rev. B*, 1994, **50**, 704–707.
102 P. A. Alekseev, J.-M. Mignot, E. V. Nefeodova, K. S. Nemkovski, V. N. Lazukov, N. N. Tiden, A. P. Menushenkov, R. V. Chernikov, K. V. Klementiev, A. Ochiai, A. V. Golubkov, R. I. Bewley, A. V. Rybina and I. P. Sadikov, *Phys. Rev. B*, 2006, **74**, 035114.
103 J. Arvanitidis, K. Papagelis, S. Margadonna and K. Prassides, *Dalton Trans.*, 2004, 3144–3146.
104 Y. W. Long, N. Hayashi, T. Saito, M. Azuma, S. Muranaka and Y. Shimakawa, *Nature*, 2009, **458**, 60–63.
105 W.-T. Chen, Y. Long, T. Saito, J. P. Attfield and Y. Shimakawa, *J. Mater. Chem.*, 2010, **20**, 7282–7286.
106 Y. Sun, C. Wang, Y. Wen, K. Zhu and J. Zhao, *Appl. Phys. Lett.*, 2007, **91**, 231913.
107 K. Gautam, D. K. Shukla, S. Francoual, J. Bednarcik, J. R. L. Mardegan, H.-P. Liermann, R. Sankar, F. C. Chou, D. M. Phase and J. Strempfer, *Phys. Rev. B*, 2017, **95**, 144112.
108 A. W. Sleight, *Curr. Opin. Solid State Mater. Sci.*, 1998, **3**, 1288–131.

109 G. D. Barrera, J. A. O. Bruno, T. H. K. Barron and N. L. Allan, *J. Phys.: Condens. Matter*, 2005, **17**, R217–R252.

110 C. Lind, *Materials*, 2012, **5**, 1125–1154.